

# Physica Status Solidi B: Basic Solid State Physics

## Ultrafast Exciton and Trion Dynamics in High-Quality Encapsulated MoS2 Monolayers

--Manuscript Draft--

<b>Manuscript Number:</b>	
<b>Article Type:</b>	Research Article
<b>Corresponding Author:</b>	Armando Genco, Ph.D Politecnico di Milano Milano, ITALY
<b>Corresponding Author E-Mail:</b>	Armando.genco@polimi.it
<b>Order of Authors:</b>	Armando Genco, Ph.D Chiara Trovatello Charalambos Louca Kenji Watanabe Takashi Taniguchi Alexander I. Tartakovskii Giulio Cerullo Stefano Dal Conte
<b>Keywords:</b>	Transitional Metal Dichalcogenides; Ultrafast Microscopy; Exciton Dynamics
<b>Section/Category:</b>	ICPS 2022: Advances in Physics of Semiconductors
<b>Abstract:</b>	<p>The extreme confinement and reduced screening in monolayer Transition Metal Dichalcogenides (TMDs) leads to the appearance of tightly bound excitons which can also couple to free charges, forming trions, owing to strong Coulomb interactions. Low temperatures and encapsulation in hexagonal Boron Nitride (hBN) narrow the excitonic linewidth, approaching the regime of homogeneous broadening, mostly dominated by the radiative decay. Ultrafast spectroscopy is a perfect tool to study exciton formation and relaxation dynamics in TMD monolayers. However, high-quality hBN-encapsulated structures have usually lateral sizes of the order of a few microns, calling for the combination of high spatial and temporal resolution in pump-probe experiments. Here we use a custom broadband pump-probe optical microscope to measure the ultrafast dynamics of neutral and charged excitons in high-quality hBN-encapsulated monolayer MoS<sub>2</sub> at 8K. Neutral excitons exhibit a narrow linewidth of 7.5 meV, approaching the homogeneous limit, which we relate to the fast recombination time of ~130 fs measured in pump-probe. Moreover, we observe markedly different dynamics of the trions over the neutral ones. Our results provide novel insights on the exciton recombination processes in TMD monolayers, paving the way for exploring the ultrafast behaviour of excitons and their many-body complexes in TMDs heterostructures.</p>
<b>Suggested Reviewers:</b>	Deborah Prezzi NANO CNR: Istituto Nanoscienze Consiglio Nazionale delle Ricerche deborah.prezzi@nano.cnr.it  Giancarlo Soavi Universitat Jena: Friedrich-Schiller-Universitat Jena giancarlo.soavi@uni-jena.de  Stefan Lochbrunner Universitat Rostock stefan.lochbrunner@uni-rostock.de  Juan Cabanillas González IMDEA Nanociencia: Fundacion IMDEA Nanociencia juan.cabanillas@imdea.org  Kenneth Knappenberger

	Penn State Eberly College of Science: The Pennsylvania State University Eberly College of Science klk260@psu.edu
<b>Opposed Reviewers:</b>	
<b>Author Comments:</b>	
<b>Additional Information:</b>	
<b>Question</b>	<b>Response</b>
Please submit a plain text version of your cover letter here.	<p>Dear Editor,</p> <p>please find attached a manuscript entitled “Ultrafast Exciton and Trion Dynamics in High-Quality Encapsulated MoS2 Monolayers”, which we would like to submit for consideration as a Research Article in Physica Status Solidi (b), following your invitation (Special Issue Invitations pssb.202200244 (inviting editor: Stefan Hildebrandt) ICPS 2022: Advances in Physics of Semiconductors).</p> <p>Low temperatures and encapsulation in hexagonal Boron Nitride (hBN) can narrow down the excitonic linewidth in Transitional Metal Dichalcogenides (TMDs) monolayers, approaching the regime of homogeneous broadening, mostly dominated by the radiative decay component. The high quality of encapsulated TMDs enables the observation of a hydrogen-like Rydberg series of excitonic states below the free particle bandgap. TMD excitons can also be dressed by a Fermi sea of free charges generated in the material due to natural or artificial doping, forming three-particle bound states (trions) in presence of low doping levels, or manifesting emerging many-body phenomena at elevated doping regimes. Ultrafast pump-probe spectroscopy has the capability to accurately measure formation and relaxation dynamics of excitons in TMD monolayers. However, high-quality hBN-encapsulated structures have usually lateral sizes of the order of a few microns, calling for the necessity of high spatial and temporal resolution in pump-probe experiments in order to properly assess exciton dynamics.</p> <p>In our work, we measure the non-equilibrium optical response of neutral and charged excitons in high-quality hBN-encapsulated monolayer MoS2 at 8K. To this aim, we developed a custom pump-probe microscopy setup with high temporal resolution, broad spectral coverage and pump energy tunability, which allows us to study samples with lateral size of few microns, performing full static and transient optical characterizations. Pumping the system above the bandgap, the neutral excitons revealed distinct multi-exponential dynamics characterized by an ultrafast formation, a fast decay, which we ascribe to direct recombination processes, and a slower one, related to carrier cooling. Neutral excitons exhibit a narrow linewidth of 7.5 meV, approaching the homogeneous limit, which we relate to the fast recombination time of <math>\approx 130</math> fs measured in pump-probe. Moreover, we investigated the trions dynamics, present in the structure due to a modest natural doping, showing the predominance of photo-induced absorption in the transient reflectivity spectra and a much longer formation time compared to neutral excitons.</p> <p>Our results provide novel insights on the exciton recombination processes in TMD monolayers and pave the way for exploring the ultrafast behaviour of excitons and their many-body complexes in high-quality TMDs heterostructures. For these reasons, we believe that the paper will be appropriate for the readership of PSS (b).</p> <p>Yours faithfully,</p>

	Armando Genco on behalf of all co-authors
Do you or any of your co-authors have a conflict of interest to declare?	No. The authors declare no conflict of interest.

# 1 Ultrafast Exciton and Trion Dynamics in High-Quality Encapsu- 2 lated MoS<sub>2</sub> Monolayers

3 *Armando Genco\** *Chiara Trovatello* *Charalambos Louca* *Kenji Watanabe* *Takashi Taniguchi* *Alexan-*  
4 *der I. Tartakovskii* *Giulio Cerullo* *Stefano Dal Conte\*\**

5 A. Genco, C. Trovatello, G. Cerullo, S. Dal Conte

6 Dipartimento di Fisica, Politecnico di Milano, Milano, MI, 20133, Italy

7 C. Trovatello

8 Present address: Department of Mechanical Engineering, Columbia University, New York, New York  
9 10027, United States.

10 C. Louca, A. I. Tartakovskii

11 Department of Physics and Astronomy, University of Sheffield, Sheffield, S3 7RH, United Kingdom

12 K. Watanabe, T. Taniguchi

13 Advanced Materials Laboratory, National Institute for Materials Science, 1-1 Namiki, Tsukuba, 305-  
14 0044, Japan

15 *Email Address: \*armando.genco@polimi.it, \*\*stefano.dalconte@polimi.it*

16 **Keywords:** *Transitional Metal Dichalcogenides, Ultrafast Microscopy, Exciton Dynamics*

17 The extreme confinement and reduced screening in monolayer Transition Metal Dichalcogenides (TMDs) leads to the appearance of  
18 tightly bound excitons which can also couple to free charges, forming trions, owing to strong Coulomb interactions. Low temperatures  
19 and encapsulation in hexagonal Boron Nitride (hBN) can narrow the excitonic linewidth, approaching the regime of homogeneous  
20 broadening, mostly dominated by the radiative decay. Ultrafast spectroscopy is a perfect tool to study exciton formation and relaxation  
21 dynamics in TMD monolayers. However, high-quality hBN-encapsulated structures have usually lateral sizes of the order of a few  
22 microns, calling for the combination of high spatial and temporal resolution in pump-probe experiments. Here we use a custom  
23 broadband pump-probe optical microscope to measure the ultrafast dynamics of neutral and charged excitons in high-quality hBN-  
24 encapsulated monolayer MoS<sub>2</sub> at 8K. Neutral excitons exhibit a narrow linewidth of 7.5 meV, approaching the homogeneous limit,  
25 which we relate to the fast recombination time of  $\approx 130$  fs measured in pump-probe. Moreover, we observe markedly different dynamics  
26 of the trions over the neutral ones. Our results provide novel insights on the exciton recombination processes in TMD monolayers,  
27 paving the way for exploring the ultrafast behaviour of excitons and their many-body complexes in TMDs heterostructures.

## 28 **1 Introduction**

29 Monolayers of transition metal dichalcogenides (1L-TMDs) are promising semiconductors with unique  
30 electrical and optical properties. The quantum confinement experienced by electrons and holes in the two-  
31 dimensional (2D) structure and the reduced Coulomb screening lead to the appearance of direct bandgap  
32 excitonic transitions showing high binding energies (up to 0.5 eV) and very large oscillator strengths up  
33 to room temperature [1, 2, 3]. Moreover, the breaking of spatial inversion symmetry in the 2D lattice  
34 and the large spin-orbit coupling generate spin-valley locked excitons at the K and K' valleys, optically  
35 addressable by circularly polarized light [4]. The strong Coulomb interactions in atomically thin TMDs  
36 also enhance the stability of many-body complexes resulting from the correlations of excitons with charge  
37 carriers. In this case, TMD excitons are dressed by a Fermi sea of free charges generated in the material by  
38 natural or artificial doping, forming three-particle bound states (trions) in presence of low doping levels,  
39 or manifesting emerging many-body phenomena at elevated doping regimes [5, 6, 7].

40 1Ls TMDs also offer the tremendous advantage of being stackable to form van der Waals heterostructures  
41 (HSs), with atomically perfect interfaces without any lattice mismatch limitation [8]. This allows to  
42 sandwich the 1Ls between few-layers of transparent high bandgap hBN, ensuring a good protection from  
43 external contaminants and dielectric insulation. hBN encapsulation has proven to be a key requirement  
44 for obtaining good optical quality from small flakes of mechanically exfoliated TMD 1Ls [9, 10]. Cryogenic  
45 temperatures and encapsulation in hBN narrow the exciton lines [11], reaching the homogeneous linewidth  
46 regime, in which the dephasing rate is dominated by radiative recombination [12]. The high quality  
47 of encapsulated TMDs reveals a hydrogen-like Rydberg series of excitonic states below the free particle  
48 bandgap [13]. In addition, the encapsulation of TMD bilayers recently allowed to unveil hybridized intra-  
49 inter layer excitonic species [14, 15], showing new types of many-body interactions [16].

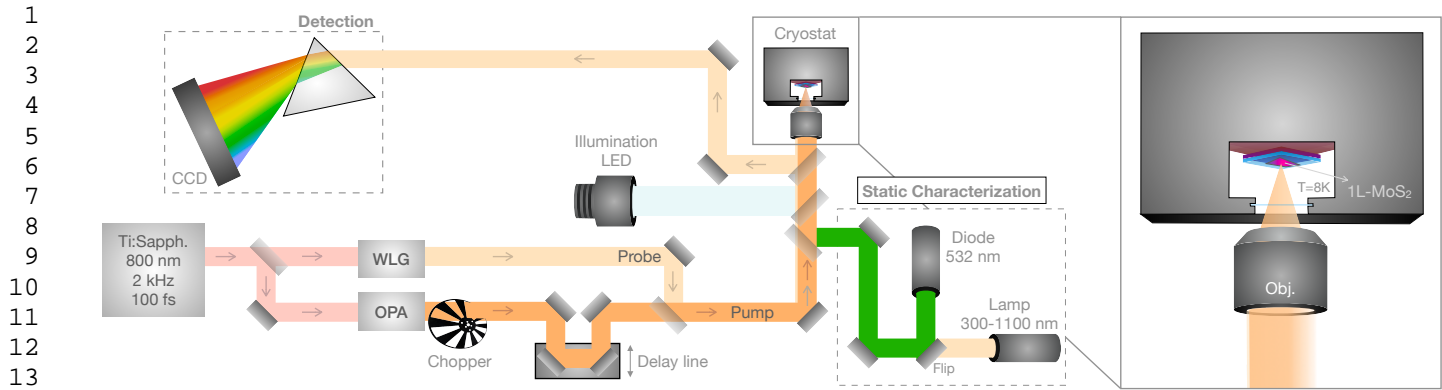


Figure 1: Sketch of the custom pump-probe microscopy setup used in our experiments. Auxiliary light sources can be coupled to the objective lens in order to perform static optical characterizations of the sample (PL and RC). Inset: schematic view of the sample placed in a closed-loop He cryostat.

Femtosecond pump-probe spectroscopy [17, 18, 19], is a powerful technique to measure the temporal dynamics of excitons in 1L TMDs. Using this technique, the photoinduced modifications of the excitonic absorption spectrum are monitored in real time. In this way a full picture of the exciton dynamics is revealed, observing in particular their build-up and decay times. The non-equilibrium optical response of neutral and charged excitons in TMDs has been previously investigated by ultrafast optical spectroscopy, focusing the study on the fundamental mechanisms that determine exciton formation [20], dissociation and decay processes [21]. However, very few works studied in details the ultrafast dynamics of TMD excitons and their many-body complexes in small area encapsulated samples, since achieving simultaneously a good temporal and spatial resolution in pump-probe experiments is challenging.

In this work we study the non-equilibrium optical response in hBN-encapsulated monolayer MoS<sub>2</sub>, with very narrow excitonic linewidths, approaching the homogeneous broadening regime. We develop a custom pump-probe microscopy setup with high spatial and temporal resolution, broad spectral coverage and pump energy tunability, which allows us to study samples with lateral size of few microns, performing full static and transient optical characterizations. Pumping the system above the bandgap, the neutral excitons reveal distinct dynamics characterized by an ultrafast formation, a fast decay, which we ascribe to direct recombination processes, and a slower one, related to carrier cooling. Trions are also observed in the sample due to residual natural doping, showing different formation and relaxation dynamics compared to neutral excitons.

## 2 Experimental

We use broadband femtosecond pump-probe microscopy to measure the ultrafast dynamics of excitons and trions in hBN-encapsulated 1L MoS<sub>2</sub> at low temperature (8K). We developed a custom confocal microscope (Fig. 1), equipped with a closed loop He cryostat, capable of transient reflectivity measurements, with high spatial and temporal resolution, as well as static reflectance contrast (RC) and photoluminescence (PL) characterizations.

For the transient measurements, we use broadband ultrashort frequency tunable visible pump and probe pulses, that are delivered collinearly on the focusing objective, resulting in a  $\approx 3 \mu\text{m}$  diameter spot on the sample. Our setup is powered by an amplified Ti:sapphire laser generating 100-fs pulses at 800 nm (1.55 eV) with 2 mJ energy and 2 kHz repetition rate. A fraction of the laser output is used to drive a non-collinear optical parametric amplifier (NOPA) pumped at 400 nm (3.1 eV) by the second harmonic of the laser, generating broadband visible pulses [22]. The chirp of the pump pulses, mainly due to dispersive glass elements present in the setup (lenses, beam splitters, filters), is compensated by using chirped mirrors [23], which compress the NOPA pulses down to  $\approx 40$  fs. The pump pulses are modulated by a mechanical chopper at 250 Hz frequency. For the broadband probe pulses, a white-light continuum is generated by

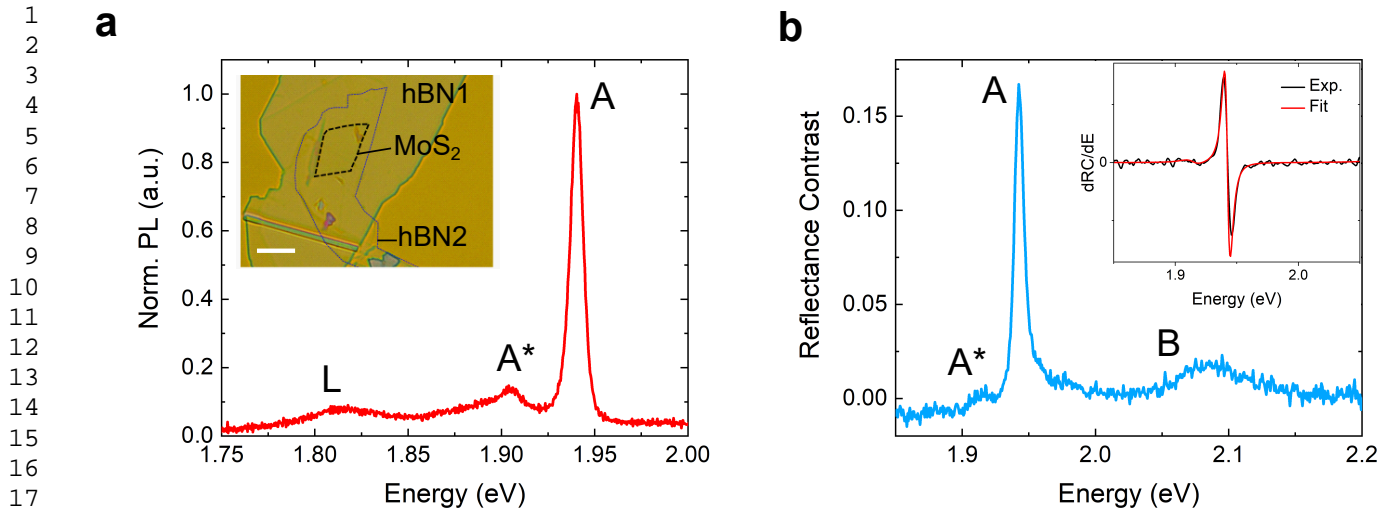


Figure 2: **a)** PL spectrum at 8K of the 1L MoS<sub>2</sub> excited with a CW 532 nm diode laser displaying a bright A exciton peak and weaker signals from trions (A\*) and localized states (L) at lower energies. Inset: bright field microscope image of the 1L MoS<sub>2</sub> (outlined by the black dashed line) encapsulated in hBN. Scale bar: 10 μm. **b)** Static RC spectrum (blue line) recorded at 8K using a tungsten lamp, evidencing the absorption features of the neutral A and B excitons and the A\* trions. Inset: Derivative of the RC spectrum (black line) fitted by a TMM model including Lorentzian oscillators (red curve).

focusing the 800 nm output of the main laser on a 1-mm-thick sapphire plate [24]. The probe beam is sent to a mechanical delay line which controls the delay between pump and probe pulses. We underline that the separate branches for pump and probe pulse generation provide a great flexibility in the choice of pump wavelength (tuned by the NOPA) and probe spectral window, which are completely independent. The pump and probe pulses are then collinearly combined by a thin wedged beam splitter and focused on the sample using an achromatic objective with 8 mm focal length (NA: 0.3). The sample is mounted in a closed-cycle helium cryostat reaching a temperature of 8K. The spatial overlap of the sample with the collinear pump and probe beams is obtained by a three-axis (xyz) translation stage coupled to a home-built imaging system consisting of a white LED for the illumination and a CMOS camera (not shown) included in the optical path. In order to measure the differential reflectivity ( $\Delta R/R$ ) spectra, the probe beam reflected by the sample is collected by the objective lens and delivered, via an additional beam splitter, to a dispersive spectrometer with a high sensitivity CCD. The setup is also equipped with a CW 532 nm diode laser and a fiber-coupled broadband tungsten white lamp for the static optical characterization of the sample (PL and RC). For pump-probe and PL measurements, a set of long-pass and short-pass filters is used to cut out the excitation light from the signal.

The sample was fabricated using a polymethylmethacrylate (PMMA)-assisted transfer method [25] by sandwiching a MoS<sub>2</sub> 1L between two thin hBN layers (45 nm bottom hBN1, 5 nm top hBN2), then placing it on a substrate. The top and bottom hBN layers provide a complete encapsulation which fully covers the area of the MoS<sub>2</sub> flake. Flakes of few-layers hBN and 1Ls of MoS<sub>2</sub> were obtained by mechanical exfoliation of bulk crystals. For the substrate, we use a dielectric mirror with a stop-band 600 meV broad and centered at 1.984 eV, terminating with a SiO<sub>2</sub> layer, in order to maximize the reflected probe intensity, crucial to obtain clean pump-probe measurements with a high signal-to-noise ratio. The inset of Figure 2a shows a bright field microscope image of the encapsulated 1L MoS<sub>2</sub>.

### 3 Results and Discussion

Fig. 2a shows the PL spectrum of the encapsulated MoS<sub>2</sub> 1L, measured at 8K exciting the sample with a CW 532 nm laser at 40 μW. The bright and sharp peak at 1.94 eV is related to the emission of the A excitons, observed together with a weaker peak at 1.905 eV, ascribed to emission from the trions (A\*). It is worth noting that such low trion absorption/PL signal is usually observed in 1L TMDs with a modest level of natural doping [6]. At much lower photon energies, a broad and weak peak appears in the PL spectrum,

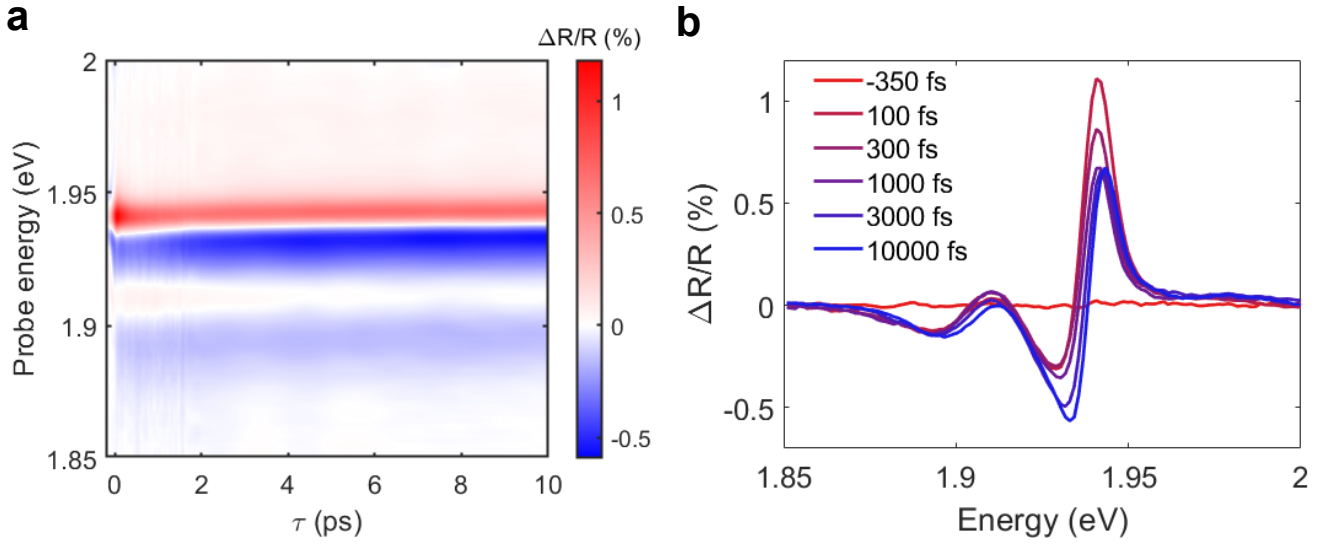


Figure 3: **a)** Color map of the  $\Delta R/R$  signal measured on the encapsulated MoS<sub>2</sub> monolayer at 8K as a function of delay time  $\tau$  and probe photon energy, pumping the sample above bandgap (2.3 eV). **b)** Spectral cross-sections of the  $\Delta R/R$  map taken at different times, showing positive and negative signals in the spectral window of the A exciton and A\* trion of the MoS<sub>2</sub> monolayer.

probably due to emission from localized states, labeled generically as L, generated by small residual strain or defects arising from the fabrication process [26].

A broadband incoherent white light source was used to measure the static RC spectrum of the encapsulated MoS<sub>2</sub> 1L at cryogenic temperatures (8K), shown in Fig. 2b. The RC spectrum is calculated as  $RC = (R_{\text{sub}} - R_{\text{1L}})/R_{\text{sub}}$ , where  $R_{\text{1L}}$  is reflectance of the sample, while  $R_{\text{sub}}$  is the reflectance taken from an area with only the two hBN layers on the substrate. In RC measurements we clearly observe one intense and narrow peak at 1.942 eV associated to the absorption of the neutral A excitons, formed by electrons and holes in the bands minima giving the lowest-energy allowed optical transition. A weaker signal related to the trion appears red shifted by about 30 meV from the A exciton. At higher energies, we observe the B excitons at 2.085 eV. We fit the derivative of the RC spectrum (black line in the inset of Fig. 2b) using the Transfer Matrix Method (TMM). This method allows to reconstruct the dielectric function of the TMD, which has been modelled by the sum of three Lorentz oscillators once the thickness and the refractive index of the other layers of the structure is known [27]. Exploiting this approach we can precisely extract the effective absorption of the material, finding a very narrow linewidth of 7.6 meV for A exciton, approaching the homogeneous limit [9] and 20 meV for A\* trion.

In order to study the temporal dynamics of excitons and trions in 1L MoS<sub>2</sub>, we photoexcite the material with pump pulses tuned at 2.34 eV, above its bandgap. For this experiment, we set the pump fluence to 80  $\mu\text{J}/\text{cm}^2$ , below the threshold for the Mott transition [28]. We record a differential reflectivity spectrum ( $\Delta R/R = (R_{\text{PumpOn}} - R_{\text{PumpOff}})/R_{\text{PumpOff}}$ ) at each delay time  $\tau$ , obtaining the map shown in Fig. 3a. Immediately after time zero, both positive and negative signals appear in the  $\Delta R/R$  map. In our experimental configuration, the positive (i.e. photobleaching) and negative features (photoinduced absorption) are attributed to pump-induced modification of the excitonic resonance (i.e. reduction of oscillator strength, broadening and shift in energy).

Fig. 3b shows the spectral cross-section of the  $\Delta R/R$  map at different delay times, displaying how the  $\Delta R/R$  spectrum changes with  $\tau$ . We can clearly resolve narrow spectral features in the energy region of the A excitons and A\* trions. Already after 100 fs a derivative-shaped signal appears in the spectral region of both the excitonic species, at about 1.94 and 1.91 eV. Around the A-exciton resonance, the  $\Delta R/R$  signal exhibits a significant absorption bleaching (i.e. red region in the map) at small delay times, which arises from the reduction of the excitonic oscillator strength due to Pauli blocking effect [29, 30]. The negative signal (i.e. blue region in the map) on the low energy side of the A exciton could be the result of the energy renormalization of the exciton due to the transient reduction of the Coulomb screening [31] or the formation of biexcitons. While for A exciton the bleaching signal is very strong at all the delay times, for

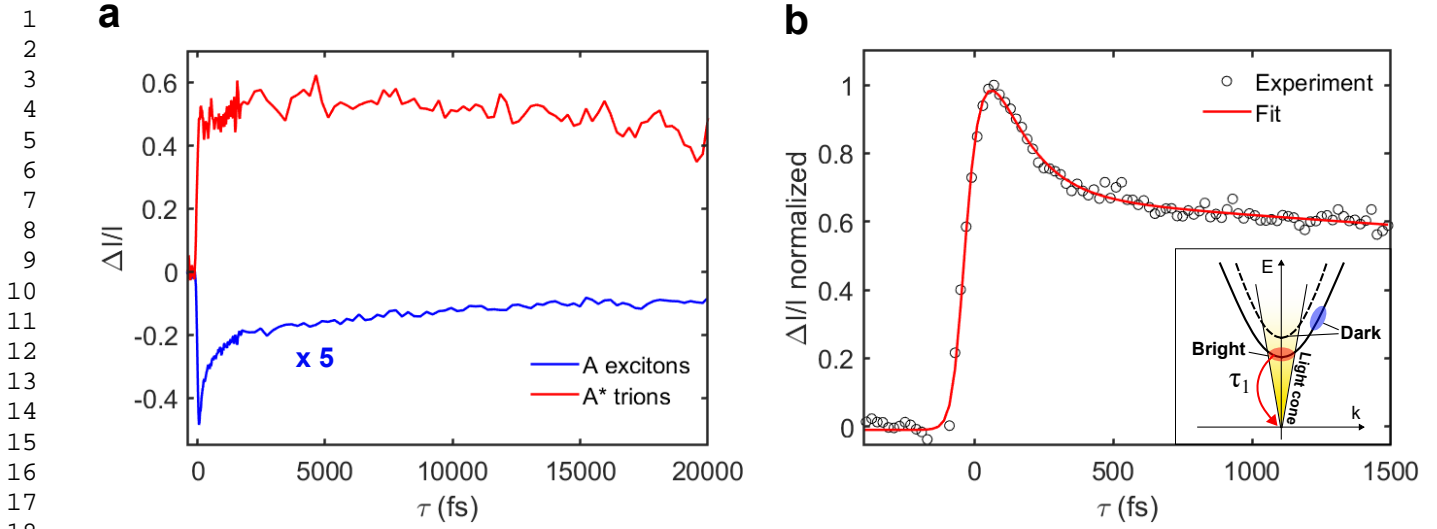


Figure 4: **a)** Temporal dynamics of the oscillator intensity variation of the excitonic species with respect to their value at the equilibrium ( $\Delta I/I$ ), showing the bleaching and the photo-induced absorption for A excitons and A\* trions, respectively. The A excitons trace is multiplied by a factor of 5. **b)** Normalized ultrafast variation of the A excitons oscillator intensity with respect to the equilibrium (black circles), fitted with a multi-exponential function (red curve), shown up to 1.5 ps. Inset: sketch of the A excitons energy-momentum dispersion showing the bright excitons recombination process ( $\tau_1$ ).

trions, the photo-induced absorption is predominant. This behaviour can be explained considering the RC static spectrum of Fig. 2b, where the trions peak is much less pronounced than that of the neutral excitons, being indicative of the low static doping in this sample, which also leads to a weaker trion bleaching signal. On the other hand, the free electron or hole carriers generated by the pump contribute to the formation of trions in the dynamic absorption spectrum, manifesting as a strong photo-induced absorption signal near the A\* resonance. Recently, this effect has been also observed in encapsulated WSe<sub>2</sub> monolayers. [32]

Figure 4a shows the oscillator intensity variation with  $\tau$  of the excitonic species with respect to their value at the equilibrium ( $\Delta I/I$ ), for A and A\*. In order to extract the dynamics of this parameter, we follow a procedure shown very recently [33], fitting for each delay time the reconstructed transient reflectivity spectrum using the TMM, then tracking the exciton peak intensity variation. Neutral excitons show a very rapid formation, followed by a multi-exponential decay with a fast component in the sub-ps time scale and a longer one. A zoom of the experimental A excitons dynamics up to 1.5 ps is shown in Fig. 4b, together with a fitted multi-exponential function convoluted with a Gaussian taking into account the instrumental response function of the apparatus. The decay times extracted from the fit are  $\tau_1 \approx 133 \pm 37$  fs,  $\tau_2 \approx 10.7 \pm 3.1$  ps, with an almost instantaneous rise time, in agreement with the formation dynamics previously measured in non-encapsulated MoS<sub>2</sub> 1L samples [20]. In fact, it has been demonstrated that the short exciton formation timescale is the result of the ultrafast exciton cascade process upon carrier photoexcitation at high energy [34]. The first rapid decay time ( $\tau_1$ ) of the A excitons can be ascribed to the combination of radiative and non-radiative direct relaxation processes of particles with small in-plane momenta which can couple to light (see the inset of Fig. 4b) [35, 36]. The homogeneous linewidth  $\gamma = FWHM/2$  is linked to exciton lifetime  $T_1$  through  $\gamma = \hbar/T_2 = \hbar/(2*T_1) + \gamma^*$ , where  $T_2$  is the coherence time and  $\gamma^*$  is related to pure dephasing processes [37]. In encapsulated TMD samples at low temperatures, the measured absorption linewidth approaches the limit of homogeneous broadening, where the coherence time is mostly dominated by the radiative lifetime of the excitonic transitions [12]. Moreover, looking at the homogeneous linewidth of non-encapsulated 1L TMDs by performing 2D electronic spectroscopy, it has been shown that at low temperatures and small exciton densities  $\gamma^*$  is very small [38]. In our case, the coherence time  $T_2$  calculated from the absorption linewidth is  $T_2 = 2\hbar/FWHM \approx 175$  fs, suggesting that the observed fast exciton decay is mostly radiative. Our measured  $\tau_1$  matches also quite well with previous theoretical calculations of the radiative lifetime for A excitons with small in-plane momenta in 1L MoS<sub>2</sub> [35]. The second, longer decay time of A excitons can be instead attributed to different processes related to incoherent exciton dynamics: carrier cooling from higher lying energy states at high in-plane momenta

1 via carrier-phonon scattering [35, 39] or slow carrier recombination from dark or defect states [40, 41].

2 On the other hand, photo-induced trions exhibit completely different dynamics compared to A excitons  
 3 (Fig. 4a). After a fast rise comparable to the build-up of A excitons, probably related to many-body  
 4 effects, we observe a delayed build-up of the signal, which reaches the maximum intensity only at about 5  
 5 ps. This effect can be related to the formation dynamics of the trion [42]. The trions decay dynamics also  
 6 appear to be longer than that of the neutral excitons. This suggests that the larger Bohr radius, the lower  
 7 binding energy and the localization of the charged particles might play a major role in both the formation  
 8 and recombination slow dynamics. It is well known that the excitons/trions recombination time is strongly  
 9 affected by those parameters. Moreover, it has been argued that long trion formation times are also related  
 10 to the small binding energy and therefore to the strength of the screened Coulomb interactions, among  
 11 other factors, including excitation power, doping density and localization length [42].  
 12  
 13  
 14

## 16 4 Conclusions

19 In summary, we measured the low-temperature (8K) ultrafast dynamics of excitons and trions in high qual-  
 20 ity hBN-encapsulated monolayer MoS<sub>2</sub>, with linewidths approaching the homogeneous broadening limit.  
 21 We developed a custom confocal pump-probe microscopy setup to investigate samples with lateral size of  
 22 few microns, performing transient reflectivity measurements with high spatial and temporal resolution and  
 23 static optical characterizations on the same spot. We observed a very narrow linewidth of 7.5 meV for the  
 24 neutral A excitons, revealing their distinct dynamics characterized by an ultrafast formation, a fast and a  
 25 slow decay. We could relate the fast exciton relaxation time to direct recombination processes, probably  
 26 dominated in this sample by radiative decay. Moreover, we investigated the trions dynamics, present in  
 27 the structure due to a modest natural doping, showing the predominance of photo-induced absorption in  
 28 the transient reflectivity spectra and a much longer formation time compared to neutral excitons.  
 29

31 The rich behaviour of neutral and charged excitons explored in our work offers novel insights on the  
 32 many-body physics of monolayer TMDs and opens up their exploitation for fundamental studies and opto-  
 33 electronic applications. Further investigations will be focused on the analysis of such encapsulated TMD  
 34 monolayers embedded in gated structures, investigating the ultrafast dynamics of excitons in elevated  
 35 doping regimes. In the future, the combination of our transient absorption microscope and high quality  
 36 TMD samples will also enable the analysis of the ultrafast dynamics of excited Rydberg excitons.  
 37  
 38

## 39 Acknowledgements

40 A.G. and G.C. acknowledge support by the European Union Horizon 2020 Programme under grant  
 41 agreement no. 881603 Graphene Core 3 and by the European Union Marie Skłodowska-Curie Actions  
 42 (project ENOSIS H2020-MSCA-IF-2020-101029644). S.D.C. acknowledge financial support from MIUR  
 43 through the PRIN 2017 Programme (Prot. 20172H2SC4). CL thanks the University of Sheffield for pro-  
 44 viding his PhD scholarship. CL and AIT acknowledge financial support of the European Graphene Flagship  
 45 Project under grant agreement 881603 and EPSRC grants EP/V006975/1, EP/V026496/1, EP/V034804/1  
 46 and EP/S030751/1.  
 47  
 48  
 49  
 50

## 51 References

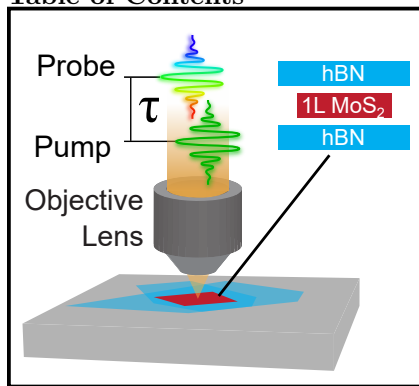
- 53 [1] K. S. Novoselov, D. Jiang, F. Schedin, T. Booth, V. Khotkevich, S. Morozov, A. K. Geim, *Proceedings*  
 54 *of the National Academy of Sciences* **2005**, *102*, 30 10451.
- 55 [2] K. F. Mak, J. Shan, *Nature Photonics* **2016**, *10*, 4 216.
- 56 [3] G. Wang, A. Chernikov, M. M. Glazov, T. F. Heinz, X. Marie, T. Amand, B. Urbaszek, *Reviews of*  
 57 *Modern Physics* **2018**, *90*, 2 021001.
- 58 [4] X. Xu, W. Yao, D. Xiao, T. F. Heinz, *Nature Physics* **2014**, *10*, 5 343.
- 59 [5] A. Imamoglu, O. Cotlet, R. Schmidt, *Comptes Rendus. Physique* **2021**, *22*, S4 1.
- 60  
 61  
 62  
 63  
 64  
 65

- [6] K. F. Mak, K. He, C. Lee, G. H. Lee, J. Hone, T. F. Heinz, J. Shan, *Nature materials* **2013**, *12*, 3 207.
- [7] M. M. Glazov, *The Journal of Chemical Physics* **2020**, *153*, 3 034703.
- [8] A. K. Geim, I. V. Grigorieva, *Nature* **2013**, *499*, 7459 419.
- [9] F. Cadiz, E. Courtade, C. Robert, G. Wang, Y. Shen, H. Cai, T. Taniguchi, K. Watanabe, H. Carrere, D. Lagarde, M. Manca, T. Amand, P. Renucci, S. Tongay, X. Marie, B. Urbaszek, *Physical Review X* **2017**, *7*, 2 1.
- [10] J. Wierzbowski, J. Klein, F. Sigger, C. Straubinger, M. Kremser, T. Taniguchi, K. Watanabe, U. Wurstbauer, A. W. Holleitner, M. Kaniber, et al., *Scientific reports* **2017**, *7*, 1 1.
- [11] O. A. Ajayi, J. V. Ardelean, G. D. Shepard, J. Wang, A. Antony, T. Taniguchi, K. Watanabe, T. F. Heinz, S. Strauf, X. Zhu, et al., *2D Materials* **2017**, *4*, 3 031011.
- [12] M. Selig, G. Berghäuser, A. Raja, P. Nagler, C. Schüller, T. F. Heinz, T. Korn, A. Chernikov, E. Malic, A. Knorr, *Nature communications* **2016**, *7*, 1 1.
- [13] A. Chernikov, T. C. Berkelbach, H. M. Hill, A. Rigosi, Y. Li, O. B. Aslan, D. R. Reichman, M. S. Hybertsen, T. F. Heinz, *Physical review letters* **2014**, *113*, 7 076802.
- [14] E. M. Alexeev, D. A. Ruiz-Tijerina, M. Danovich, M. J. Hamer, D. J. Terry, P. K. Nayak, S. Ahn, S. Pak, J. Lee, J. I. Sohn, et al., *Nature* **2019**, *567*, 7746 81.
- [15] I. C. Gerber, E. Courtade, S. Shree, C. Robert, T. Taniguchi, K. Watanabe, A. Balocchi, P. Renucci, D. Lagarde, X. Marie, et al., *Physical Review B* **2019**, *99*, 3 035443.
- [16] C. Louca, A. Genco, S. Chiavazzo, T. P. Lyons, S. Randerson, C. Trovatiello, P. Claronino, R. Jayaprakash, K. Watanabe, T. Taniguchi, et al., *arXiv preprint arXiv:2204.00485* **2022**.
- [17] G. Aivazian, H. Yu, S. Wu, J. Yan, D. G. Mandrus, D. Cobden, W. Yao, X. Xu, *2D Materials* **2017**, *4*, 2 025024.
- [18] A. Singh, G. Moody, S. Wu, Y. Wu, N. J. Ghimire, J. Yan, D. G. Mandrus, X. Xu, X. Li, *Physical review letters* **2014**, *112*, 21 216804.
- [19] Z. Wang, A. Molina-Sanchez, P. Altmann, D. Sangalli, D. De Fazio, G. Soavi, U. Sassi, F. Bottegoni, F. Ciccacci, M. Finazzi, et al., *Nano letters* **2018**, *18*, 11 6882.
- [20] C. Trovatiello, F. Katsch, N. J. Borys, M. Selig, K. Yao, R. Borrego-Varillas, F. Scotognella, I. Kriegel, A. Yan, A. Zettl, et al., *Nature communications* **2020**, *11*, 1 1.
- [21] S. Dal Conte, C. Trovatiello, C. Gadermaier, G. Cerullo, *Trends in Chemistry* **2020**, *2*, 1 28.
- [22] G. Cerullo, M. Nisoli, S. Stagira, S. De Silvestri, *Optics letters* **1998**, *23*, 16 1283.
- [23] C. Manzoni, D. Polli, G. Cerullo, *Review of scientific instruments* **2006**, *77*, 2 023103.
- [24] R. R. Alfano, *The supercontinuum laser source: the ultimate white light*, Springer, **2016**.
- [25] J. T. Mlack, P. Masih Das, G. Danda, Y.-C. Chou, C. H. Naylor, Z. Lin, N. P. López, T. Zhang, M. Terrones, A. Johnson, et al., *Scientific reports* **2017**, *7*, 1 1.
- [26] Y. Yu, J. Dang, C. Qian, S. Sun, K. Peng, X. Xie, S. Wu, F. Song, J. Yang, S. Xiao, et al., *Physical Review Materials* **2019**, *3*, 5 051001.
- [27] A. Raja, L. Waldecker, J. Zipfel, Y. Cho, S. Brem, J. D. Ziegler, M. Kulig, T. Taniguchi, K. Watanabe, E. Malic, et al., *Nature nanotechnology* **2019**, *14*, 9 832.

- 1 [28] A. Steinhoff, M. Florian, M. Rösner, G. Schönhoff, T. O. Wehling, F. Jahnke, *Nature communications*  
2 **2017**, *8*, 1 1.  
3
- 4 [29] V. Shahnazaryan, I. Iorsh, I. A. Shelykh, O. Kyriienko, *Physical Review B* **2017**, *96*, 11 115409.  
5
- 6 [30] F. Katsch, M. Selig, A. Knorr, *Physical Review Letters* **2020**, *124*, 25 257402.  
7
- 8 [31] E. A. Pogna, M. Marsili, D. De Fazio, S. Dal Conte, C. Manzoni, D. Sangalli, D. Yoon, A. Lombardo,  
9 A. C. Ferrari, A. Marini, et al., *ACS nano* **2016**, *10*, 1 1182.  
10
- 11 [32] T. Y. Jeong, S.-Y. Lee, S. Jung, K. J. Yee, *Current Applied Physics* **2020**, *20*, 2 272.  
12
- 13 [33] C. Trovatello, F. Katsch, Q. Li, X. Zhu, A. Knorr, G. Cerullo, S. Dal Conte, *Nano Letters* **2022**.  
14
- 15 [34] S. Brem, M. Selig, G. Berghaeuser, E. Malic, *Scientific reports* **2018**, *8*, 1 1.  
16
- 17 [35] H. Wang, C. Zhang, W. Chan, C. Manolatou, S. Tiwari, F. Rana, *Physical Review B* **2016**, *93*, 4  
18 045407.  
19
- 20 [36] C. Robert, D. Lagarde, F. Cadiz, G. Wang, B. Lassagne, T. Amand, A. Balocchi, P. Renucci, S. Tongay,  
21 B. Urbaszek, et al., *Physical review B* **2016**, *93*, 20 205423.  
22
- 23 [37] M. O. Scully, M. S. Zubairy, *Quantum optics*, **1999**.  
24
- 25 [38] G. Moody, C. Kavir Dass, K. Hao, C.-H. Chen, L.-J. Li, A. Singh, K. Tran, G. Clark, X. Xu,  
26 G. Berghäuser, et al., *Nature communications* **2015**, *6*, 1 1.  
27
- 28 [39] Z. Nie, R. Long, L. Sun, C.-C. Huang, J. Zhang, Q. Xiong, D. W. Hewak, Z. Shen, O. V. Prezhdo,  
29 Z.-H. Loh, *ACS nano* **2014**, *8*, 10 10931.  
30
- 31 [40] H. Wang, C. Zhang, F. Rana, *Nano letters* **2015**, *15*, 1 339.  
32
- 33 [41] T. Völzer, F. Fennel, T. Korn, S. Lochbrunner, *Physical Review B* **2021**, *103*, 4 045423.  
34
- 35 [42] A. Singh, G. Moody, K. Tran, M. E. Scott, V. Overbeck, G. Berghäuser, J. Schaibley, E. J. Seifert,  
36 D. Pleskot, N. M. Gabor, et al., *Physical Review B* **2016**, *93*, 4 041401.  
37  
38  
39  
40  
41  
42  
43  
44  
45  
46  
47  
48  
49  
50  
51  
52  
53  
54  
55  
56  
57  
58  
59  
60  
61  
62  
63  
64  
65

1  
2  
3  
4  
5  
6  
7  
8  
9  
10  
11  
12  
13  
14  
15  
16  
17  
18  
19  
20  
21  
22  
23  
24  
25  
26  
27  
28  
29  
30  
31  
32  
33  
34  
35  
36  
37  
38  
39  
40  
41  
42  
43  
44  
45  
46  
47  
48  
49  
50  
51  
52  
53  
54  
55  
56  
57  
58  
59  
60  
61  
62  
63  
64  
65

### Table of Contents



The ultrafast dynamics of excitons with narrow linewidth and trions in hBN-encapsulated monolayer MoS<sub>2</sub> have been studied using a pump-probe microscopy setup with high spatial and temporal resolution, broad spectral coverage and pump energy tunability. Excitons show an ultrafast formation, a decay with a fast component, ascribed to direct recombination processes, and a slower one, related to carrier cooling, distinctly different compared to those measured for trions.